

Ca²⁺-Mediated Synthetic Biosystems Offer Protein Design Versatility, Signal Specificity, and Pathway Rewiring

Evan Mills¹ and Kevin Truong^{1,2,*}

¹Institute of Biomaterials and Biomedical Engineering, University of Toronto, 164 College Street, Toronto, ON M5S 3G9, Canada

²Edward S. Rogers Sr. Department of Electrical and Computer Engineering, University of Toronto, 10 King's College Circle, Toronto, ON M5S 3G4, Canada

*Correspondence: kevin.truong@utoronto.ca

DOI 10.1016/j.chembiol.2011.09.014

SUMMARY

Synthetic biosystems have been engineered that enable control of metazoan cell morphology, migration, and death. These systems possess signal specificity, but lack flexibility of input signal. To exploit the potential of Ca²⁺ signaling, we designed RhoA chimeras for reversible, Ca²⁺-dependent control over RhoA morphology and migration. First, we inserted a calmodulin-binding peptide into a RhoA loop that activates or deactivates RhoA in response to Ca²⁺ signals depending on the chosen peptide. Second, we localized the Ca²⁺-activated RhoA chimera to the plasma membrane, where it responded specifically to local Ca²⁺ signals. Third, input control of RhoA morphology was rewired by coexpressing the Ca²⁺-activated RhoA chimera with Ca²⁺-transport proteins using acetylcholine, store-operated Ca²⁺ entry, and blue light. Engineering synthetic biological systems with input versatility and tunable spatiotemporal responses motivates further application of Ca²⁺ signaling in this field.

INTRODUCTION

Synthetic biosystems engineered at the molecular level have been reported that enable control of metazoan cell morphology (Levskaia et al., 2009; Yeh et al., 2007), migration (Wang et al., 2010; Wu et al., 2009), and apoptosis (Gray et al., 2010) using exogenous chemicals or light. Synthetic proteins and protein networks allow the reprogramming of cells to perform diverse tasks that they are not otherwise capable of performing. Already, reprogrammed cells are powerful tools for research in embryonic development (Wang et al., 2010), drug discovery (Gray et al., 2010), and therapeutic interventions in diseases such as leukemia (Kalos et al., 2011). These systems were designed using specific allosteric interactions such as the caging of Rac1 by LOV2 in PARac (Wu et al., 2009) or with protein domains and peptides that are responsive to specific exogenous chemicals such as rapamycin in the FRB/FKBP12 heterodimerization of SNIPer (Gray et al., 2010). These approaches provide signal specificity but necessarily limit the flexibility in providing alter-

nate input signals to these systems, such as different wavelengths of light or exogenous chemicals, without a complete redesign. Although these biosystems are hard wired to a particular input stimulus, endogenous biosystems based on Ca²⁺ signaling are inherently modular—that is, proteins responding to and transporting Ca²⁺ are interchanged and interconnected in diverse ways across cell types and subcellular locations to create signal complexity and specificity (Berridge et al., 2000).

Ca²⁺ is a ubiquitous second messenger that is involved in signaling pathways regulating cell migration, differentiation, proliferation, and death. Complexity in Ca²⁺ signaling is achieved through a variety of mechanisms including frequency decoding (De Koninck and Schulman, 1998), spatiotemporal patterning (Wei et al., 2009), and modularity (Berridge et al., 2000). Complexity through modularity is particularly powerful: for example, Ca²⁺ released from the endoplasmic reticulum through ryanodine receptor (RyR) and IP₃ receptor (IP₃R) enables troponin C-mediated contraction in skeletal muscles (Berridge, 1993), whereas RyR and IP₃R Ca²⁺ activation of calmodulin (CaM)-dependent kinase II enables long-term potentiation and depression in neurons (Berridge, 1993, 1998). Activation of the same Ca²⁺-generating system (RyR and IP₃R) can lead to different physiological processes in different cells depending on the presence of Ca²⁺-dependent proteins (troponin C or CaM-dependent kinase II). Similarly, Ca²⁺ can be mobilized in neurons using voltage (direct influx from the extracellular fluid by L-type channels) or chemicals (such as glutamate through the IP₃ pathway), both of which are involved in memory and learning (Berridge, 1998). Different systems for generating Ca²⁺ can have similar physiological effects because they enable the same or similar Ca²⁺-dependent proteins to function.

In this study, we report a way to reprogram certain mammalian cells such that several exogenous stimuli (i.e., blue light, thapsigargin, and acetylcholine) trigger blebbing morphology and cell migration. The reprogramming is done via CaM and its binding peptides (Crivici and Ikura, 1995), which translate the varied stimuli into the same physiological effect: RhoA activation leading to bleb formation and actinomyosin-based migration (Fackler and Grosse, 2008). Local Ca²⁺ signals were created using Ca²⁺-generating proteins that are specific to the plasma membrane (PM) such as α 4-acetylcholine receptor (α 4-nAChR) (Nashmi et al., 2003) or the endoplasmic reticulum (ER) such as the store-operated Ca²⁺-entry (SOCE) proteins Stim1 and Orai1 (Zhou et al., 2010a, 2010b) that enable specific activation

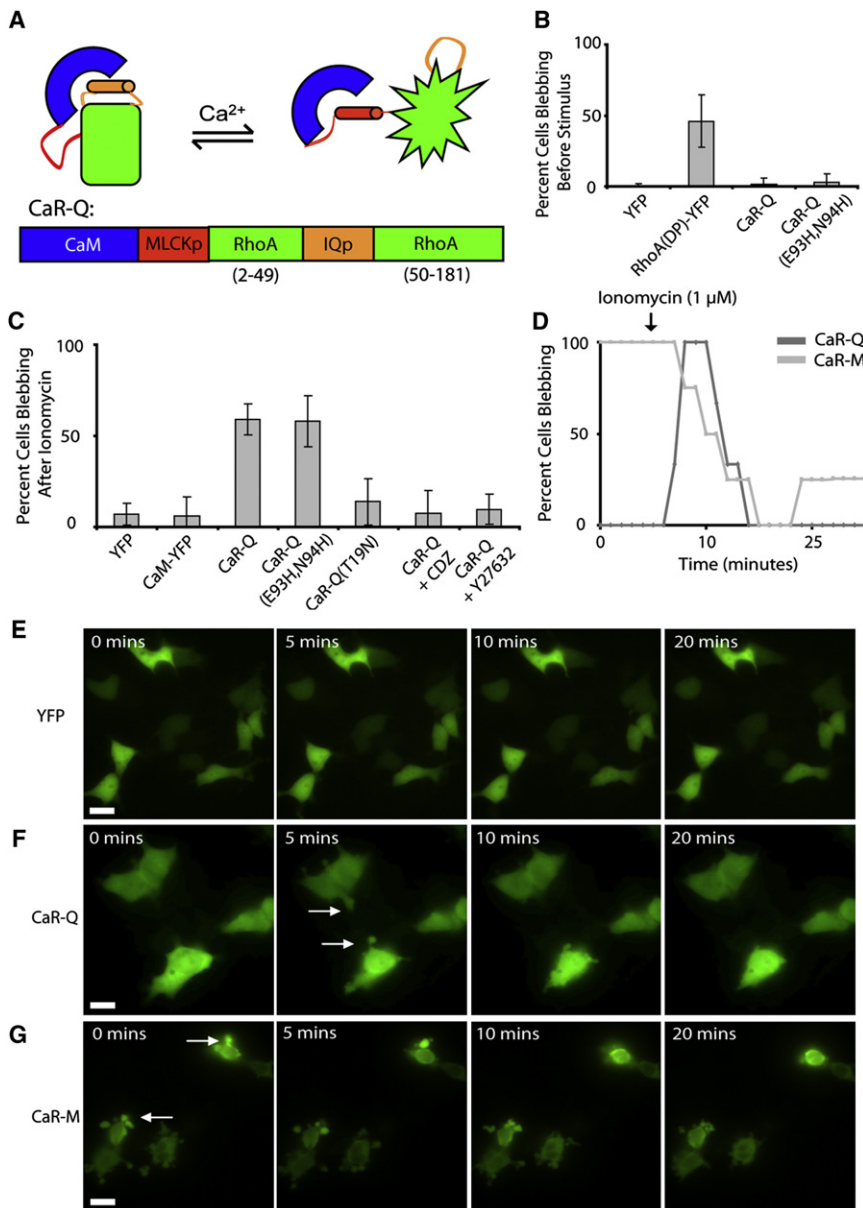


Figure 1. Design and Characterization of CaR-Q

(A) Cartoon showing CaR-Q in the absence (left) and presence (right) of Ca²⁺: RhoA (green), CaM (blue), IQp (orange), and MLCKp (red).

(B) The percent of HEK293 cells with a blebbing morphology before any stimulus, transfected with the indicated constructs (n = 10 experiments each, >100 observed cells). Data are the mean and error bars are the standard deviation.

(C) The percent of morphologically normal, CaR-Q-expressing HEK293 cells that developed a blebbing morphology after ionomycin stimulus, under the indicated transfection and inhibitor conditions (n = 3 experiments each, >10 observed cells).

(D) Time course showing blebbing morphology versus time for representative cells transfected with CaR-Q (dark line) and CaR-M (light line) after ionomycin stimulus.

(E–G) HEK293 cells transfected with YFP (E), CaR-Q (F), or CaR-M (G) were stimulated with ionomycin at 5 min, with white arrows highlighting dynamic blebs. Scale bars represent 30 μm.

See also Figure S1 and Movies S1–S3.

of the CaM/RhoA chimera. The toolbox of Ca²⁺-generating proteins used also includes channelrhodopsin-2 (ChR2), which can translate 440 nm light into cytoplasmic Ca²⁺ (Petreanu et al., 2007) and thus morphology changes and migration.

RESULTS

An Embedded Peptide Chimera Enables Ca²⁺-CaM Control over RhoA

Ca²⁺-dependent control over RhoA (a protein not normally directly sensitive to Ca²⁺) was achieved by genetically embedding CaM-binding peptides within the secondary structure of RhoA(Q63L) (Figure 1A; see Figure S1 available online). Genetically embedding peptides within a surface-exposed loop in the secondary structure of a protein allowed the chimera to bind

a new peptide-specific partner (in this case CaM) while having minimal impact on the protein's existing binding partners (specifically ROCK) in the absence of the peptide-specific partner. Introducing a synthetic CaM-binding site in RhoA enabled control over the strength and Ca²⁺ dependence of the CaM-chimera interaction, in contrast to our previous work, where the interaction was restricted to a naturally occurring CaM-binding site in RhoA (Mills et al., 2010). The surface-exposed loop in RhoA between amino acids 49 and 50 was chosen for chimera construction (Figure S1) for several reasons: first, it is sandwiched between regions of well-defined secondary structure; second, it is distal from the switch I and II regions (Hakoshima et al., 2003);

and third, it is near the N terminus in 3D space, and thus an N-terminally fused CaM can bind to any CaM-binding peptides inserted there. An IQ-motif peptide (IQp) was chosen as the embedded peptide so that CaM would bind to the RhoA/IQp chimera at resting Ca²⁺ (IQp binds CaM Ca²⁺ independently with a micromolar dissociation constant; Trybus et al., 2007). This should prevent RhoA binding to effector proteins at basal Ca²⁺. To force CaM dissociation from the chimera at high Ca²⁺, a second peptide should be available that binds CaM in a Ca²⁺-dependent manner with a stronger affinity, such as from myosin light chain kinase (MLCKp, nanomolar dissociation constant; Lukas et al., 1986). Finally, CaM was retained in the fusion to minimize the disturbance to the cell's balance of CaM and binding partners. Thus, the fusion would be CaM-MLCK-RhoA(Q63L)/IQp (Figure 1A; Figure S1). YFP was added as

a C-terminal fusion for visualization (Rekas et al., 2002); for brevity, we will refer to the construct as CaR-Q (Ca²⁺-responsive RhoA protein with IQ-motif peptide).

CaR-Q Can Mediate Ca²⁺-Sensitive Cell Morphology Changes

CaR-Q caused Ca²⁺-induced morphology changes consistent with switchable RhoA activity in several mammalian cell lines including HEK293, HeLa, and CHO cells (Figure 1; Figures S1–S3; Movies S1–S3). Ca²⁺-dependent activation of CaR-Q could not be measured *in vitro* using a rhotekin Rho-binding domain (RBD)-GST pull-down assay, likely because CaR-Q was poorly folded in *Escherichia coli*. Instead, CaR-Q was fused with a membrane localization tag and coexpressed with RBD-GST sandwiched around monomeric red fluorescent protein (mRFP); in live cells, RBD-mRFP-GST appeared to colocalize with membrane-localized CaR-Q after stimulation with ionomycin and Ca²⁺ (Figure S2). Pairs of YFP and RFP images were analyzed using the Pearson correlation (PC) coefficient before and after ionomycin stimulation. Soluble cyan fluorescent protein (CFP) was used as a spectrally distinct volume indicator (Correia et al., 2008; Robinson et al., 2002). PC correlation between RBD and CaR-Q increased by 26%, whereas the correlation change was less than 1% for the dominant-negative CaR-Q(T17N) (Figure S2). Correlation between CaR-Q and the volume indicator decreased after ionomycin stimulation, due to a less even distribution of CaR-Q possibly because of membrane ruffling, suggesting that the increased correlation was not a volumetric effect.

To assay the physiological activity of CaR-Q, we utilized the observation that overexpression of cytoplasmic RhoA(Q63L)-YFP causes dynamic nonapoptotic blebbing in certain epithelial-like cell lines such as HEK293, HeLa, and CHO (Figure 1; Figures S1 and S3). Cells expressing CaR-Q were no more likely to bleb than YFP-expressing control cells at basal Ca²⁺, and much less likely to bleb than cells expressing RhoA(Q63L)-YFP, consistent with the design of CaR-Q to suppress RhoA activity at basal Ca²⁺ (Figure 1B). When cells expressing CaR-Q were stimulated with ionomycin and Ca²⁺, these cells began to show dynamic blebs consistent with RhoA activation that were not present in control cells expressing YFP or CaM-YFP, a dominant-negative mutant of CaR-Q (RhoA-T19N), or when CaR-Q was incubated with Y-27632, an inhibitor of the RhoA effector Rho kinase, or the CaM inhibitor CDZ (Figures 1C–1F; Figures S1–S3; Movies S1 and S2). The blebbing was fully reversible, as cells returned to their normal morphology when the ionomycin transient expired (usually after 10–15 min) or upon adding EDTA to chelate free Ca²⁺ (Figures 1D–1G).

Mutations to disrupt binding between CaR-Q and GTPase-accelerating proteins (GAPs) (E93H, N94H) had little effect on either blebbing morphology at the basal level or the likelihood of blebbing induction after Ca²⁺ (Figures 1B and 1C), for both cytoplasmic and membrane-localized CaR-Q, in contrast to the reported results with PARac (Wu et al., 2009). However, the caging mechanism reported for PARac is substantially different from the CaM/peptide approach taken here; these results suggest that CaR-Q does not act as a “GAP sink.”

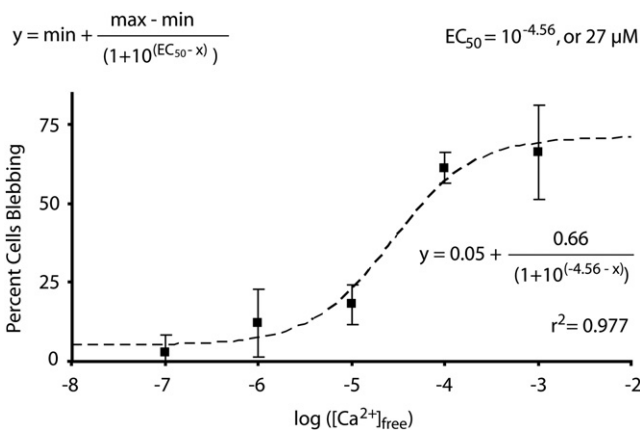


Figure 2. Determination of EC_{50} Value for Ca²⁺ Activation of CaR-Q
 EC_{50} values were determined by stimulating HEK293 cells transfected with pLyn-CaR-Q with ionomycin. Data were fit to a standard sigmoid of the form indicated at the top by minimizing the sum of squares between the fitted curve (dashed line) and the data (filled squares). The error bars are the standard deviation and $n = 3$ independent experiments each. The quality of the fit (r^2) is shown, as are the fitted coefficients. See also Figure S2.

There was a dose-dependent relationship between free Ca²⁺ and the blebbing morphology. The cell medium was buffered at specific free Ca²⁺ concentrations between 0.1 and 1,000 μ M, and the likelihood of blebbing morphology was observed after addition of ionomycin to cells expressing membrane-localized CaR-Q. The free concentration of Ca²⁺ resulting in 50% change (EC_{50}) was $10^{-4.56}$, or 27 μ M (Figure 2). The quality of the fit is good: $r^2 = 0.977$. An EC_{50} greater than 1 μ M is reasonable, because previous studies have shown that the modulation of the CaM-binding peptide interface in protein Ca²⁺ biosensors can tune the Ca²⁺ sensitivity between 0.6 and 160 μ M (Palmer et al., 2006). In our analysis, we forced the slope of the sigmoid to be 1 (i.e., it did not allow for cooperativity between Ca²⁺ binding and morphology change). With this restraint lifted, the calculated EC_{50} is only slightly different at 25 μ M.

The embedded peptide design is robust: replacing the embedded peptide with one that binds CaM in a Ca²⁺-dependent manner can reverse the direction of the Ca²⁺-induced RhoA switch (Figures 1D and 1G). To test the flexibility of our embedded peptide design, we replaced the embedded IQ-motif peptide with MLCKp and removed the N-terminally fused MLCKp to create a CaM-RhoA(Q63L)/MLCKp chimera, termed CaR-M. When CaR-M was expressed in HEK293 cells, the percentage of blebbing cells was not significantly different from cells expressing RhoA(Q63L)-YFP (49.4% \pm 18.3% and 47.2% \pm 15.0%, respectively). This is consistent with the CaR-M design to not affect RhoA activity at basal Ca²⁺ when there is little interaction between CaM and MLCKp. When cells expressing CaR-M were stimulated with ionomycin, blebbing slowed and retracted in some cells, consistent with a loss of RhoA activity (Figure 1G; Movie S3). This shows that the embedded peptide approach to synthetic protein control can create a switch in any direction (i.e., on-off or off-on), depending on the characteristic interaction between CaM and the embedded peptide.

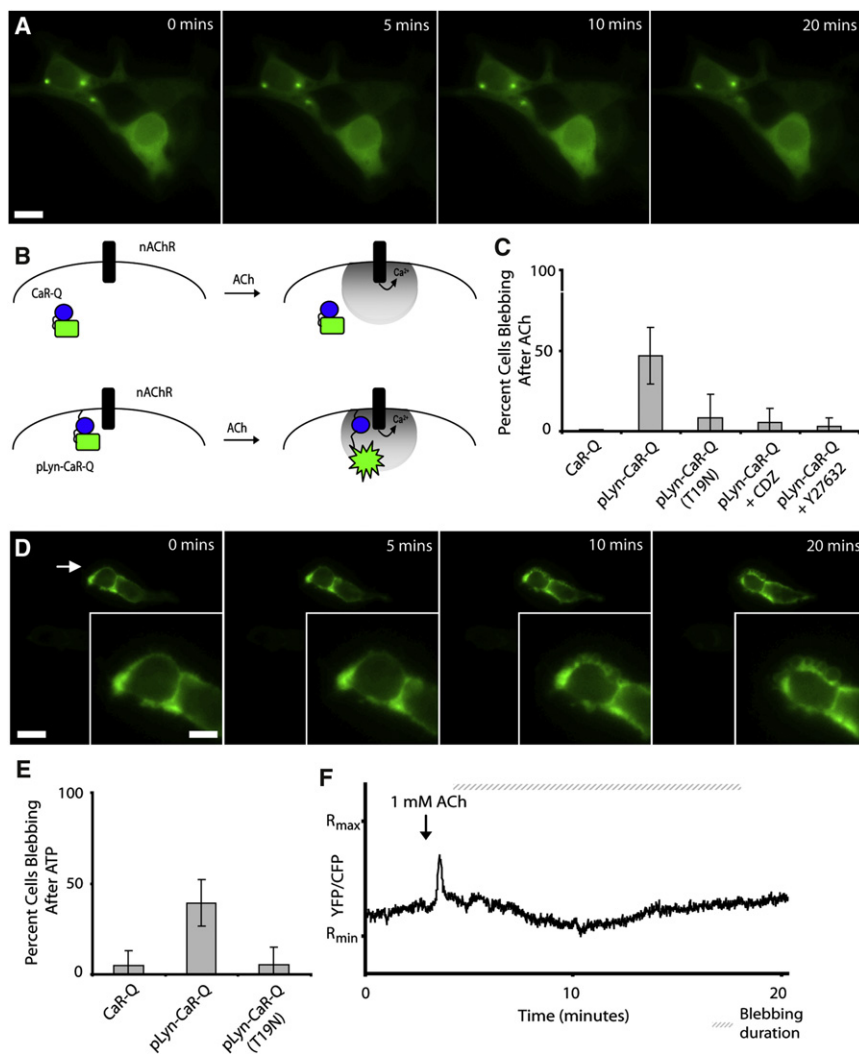


Figure 3. Modular, Local Activation of pLyn-CaR-Q

(A) HEK293 cells cotransfected with nAChR- α 4 and CaR-Q and stimulated with ACh at 5 min. The scale bar represents 30 μ m.

(B) Cartoon hypothesizing how locally high Ca²⁺ activates pLyn-CaR-Q but not CaR-Q; nAChR- α 4 (black) and CaR-Q (blue and green).

(C) The percent of morphologically normal and pLyn-CaR-Q- and nAChR- α 4-coexpressing HEK293 cells that developed a blebbing morphology after ACh stimulus, under the indicated transfection and inhibitor conditions (n = 3 experiments each, >10 observed cells). Data are the mean and error bars are the standard deviation.

(D) HEK293 cells cotransfected with nAChR- α 4 and pLyn-CaR-Q and stimulated with ACh at 5 min. The arrow highlights a region of bleb formation and indicates the area enlarged in the inset. The scale bars represent 30 μ m in the main panels and 15 μ m in the insets.

(E) The percent of morphologically normal and pLyn-CaR-Q- and nAChR- α 4-coexpressing HEK293 cells that developed a blebbing morphology after ATP stimulus, under the indicated transfection and inhibitor conditions (n = 3 experiments each, >10 observed cells).

(F) Ratio of YFP/CFP signal intensity from a representative experiment with cells cotransfected with TNXL, pLyn-CaR-Q, and nAChR- α 4. The arrow indicates when ACh was added, and the hatched line indicates the window when blebbing was observed in at least one cell.

See also Figure S3 and Movies S4–S6.

Spatially Localized Ca²⁺ Signals Can Regulate Cell Morphology via CaR-Q

CaR-Q is sensitive to local Ca²⁺ signals and can be differentially activated by different spatial patterns of Ca²⁺ signaling (Figures 3 and 4; Figure S3; Movies S4–S6). To determine whether CaR-Q could respond to short Ca²⁺ transients, in addition to long periods of high Ca²⁺ as with ionomycin, we stimulated HEK293 cells expressing CaR-Q with the exogenous stimulus acetylcholine (ACh). ACh signaling was mediated using the α 4 subunit of nAChR to create a plasma membrane Ca²⁺ channel (Nashmi et al., 2003). This experiment was also designed to test whether CaR-Q could operate as a robust Ca²⁺-signaling module, that is, to determine whether different upstream Ca²⁺-generating elements could activate CaR-Q. Cells cotransfected with nAChR- α 4 and CaR-Q did not bleb in response to ACh stimulation (Figure 3A; Movie S4). We suspected that CaR-Q may be more likely to respond to ACh on the plasma membrane given that the Ca²⁺ influx originated there, and that RhoA is localized to the plasma membrane during activation in vivo (Pertz et al., 2006). CaR-Q was fused to a membrane tag derived from Lyn kinase (see Supplemental Experimental Procedures for peptide

sequence) to create pLyn-CaR-Q (Figure 3B), and this construct reliably induced blebbing in response to ACh (Figures 3C and 3D; Movie S5). As with ionomycin, blebbing did not occur with a dominant-negative mutant of pLyn-CaR-Q (RhoA T19N), or in the presence of Y-27632 or CDZ (Figure 3C; Movie S6). Further, pLyn-CaR-Q induced blebbing when HEK293 cells were stimulated with ATP (Ca²⁺ generated by the IP₃ pathway) but CaR-Q did not (Figure 3E). To determine the temporal relationship between the Ca²⁺ signal and appearance of blebbing, cells were cotransfected with pLyn-CaR-Q, nAChR- α 4, and a FRET-based Ca²⁺ sensor, TNXL (Mank et al., 2006). These experiments showed that ACh induced a Ca²⁺ transient with a 10–20 s peak, followed by a 2–3 min delay before the onset of morphology change and then 5–15 min of blebbing morphology (Figure 3F). This shows that a short Ca²⁺ event can cause a relatively prolonged physiological change. Taken together, this set of results demonstrates that two essential features of Ca²⁺ signaling are functioning in the case of CaR-Q: first, that CaR-Q and its localized derivatives can respond to Ca²⁺ generated from several upstream modules, and second, that CaR-Q is sensitive to changes in local or global Ca²⁺, depending on its subcellular localization.

CaR-Q, when localized to the ER, can induce morphology change in response to SOCE (Figure 4; Movies S7 and S8).

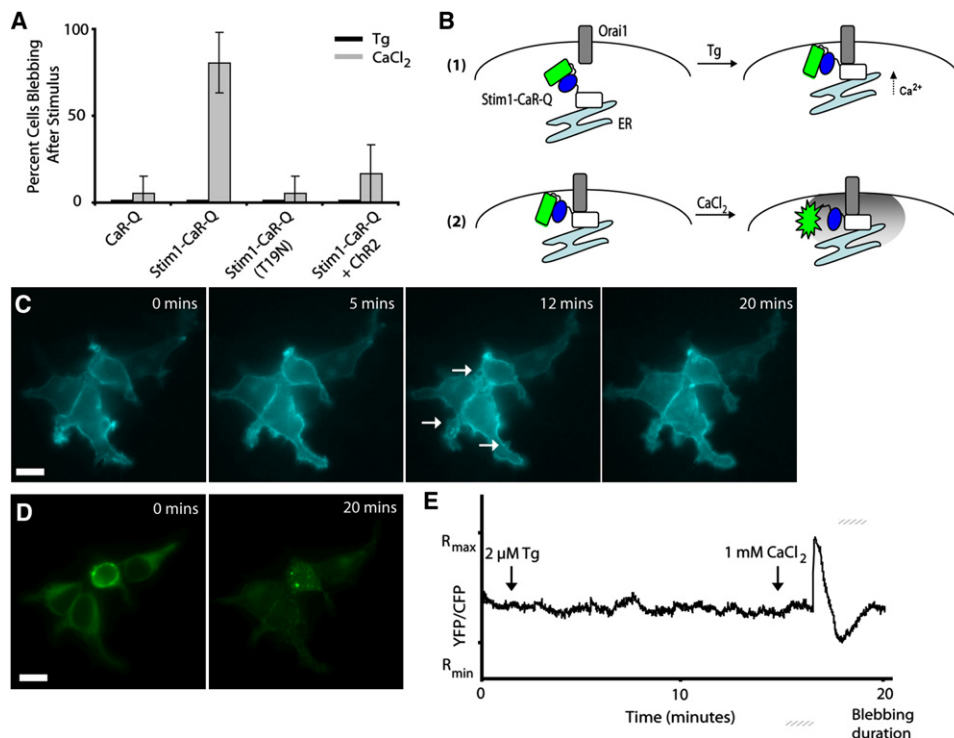


Figure 4. SOCE-Mediated Activation of Stim1-CaR-Q

(A) The percent of morphologically normal HEK293 cells that developed a blebbing morphology after Tg (dark bars) and CaCl₂ (light bars) stimulus, under the indicated transfection and inhibitor conditions (n = 3 experiments each, >10 observed cells). In the latter three conditions, cells were coexpressing Orai1-Ceru in addition to those indicated. Data are the mean and error bars are the standard deviation.

(B) Cartoon demonstrating how SOCE enables activation of Stim1-CaR-Q; Orai1 (gray), Stim1-CaR-Q (white, blue, and green), and the ER (light blue).

(C) HEK293 cells cotransfected with Orai1-Ceru and Stim1-CaR-Q were stimulated with Tg at 5 min and CaCl₂ at 10 min. The CFP channel is shown because it best outlines the plasma membrane. The arrows indicate regions of blebbing. The scale bar represents 25 μm.

(D) YFP channel of the cells in (C)–(F) before stimulus and after the experiment was completed shows the change in Stim1-CaR-Q localization. The scale bar represents 25 μm.

(E) Ratio of YFP/CFP signal intensity from a representative experiment with cells cotransfected with TNXL, Stim1-CaR-Q, and Orai1-Ceru. The arrows indicate when Tg and CaCl₂ were added and the hatched line indicates the window when blebbing was observed in at least one cell.

See also [Movies S7 and S8](#).

SOCE is a homeostatic mechanism employed by cells when the intracellular Ca²⁺ stores (e.g., in the ER lumen) are depleted (Zhou et al., 2010a, 2010b). Two proteins involved in SOCE are Stim1 and Orai1, which act as a Ca²⁺ sensor (Zhou et al., 2010a) and Ca²⁺ channel, respectively (Zhou et al., 2010b). Given that SOCE is an important physiological pathway of Ca²⁺ entry, we tested whether CaR-Q could respond to SOCE induced by thapsigargin (Tg). Cells coexpressing Orai1 and CaR-Q in Ca²⁺-free medium were stimulated with Tg and Ca²⁺, but blebbing was not observed (Figure 4A). Given our insights into the spatially sensitive nature of CaR-Q response to Ca²⁺, CaR-Q was localized to the cytoplasmic-facing membrane of the ER using Stim1 or Stim1-CaR-Q (Figure 4B). Treatment with Tg alone induced punctum formation, consistent with Stim1 and Orai1 oligomerization (Zhou et al., 2010a), but did not induce blebbing until addition of Ca²⁺ to the extracellular medium (Figures 4C and 4D; [Movie S7](#)). Blebbing did not occur in the case of a dominant-negative Stim1-CaR-Q (RhoA T19N) or when we used an alternate plasma membrane Ca²⁺ channel, Chr2 (Petreanu et al., 2007), as the source of Ca²⁺ influx for Stim1-CaR-Q (Figure 4A; [Movie S8](#)). As with the nAChR-α4

experiments, the induced SOCE experiments were repeated with a cotransfection of Stim1-CaR-Q, Orai1, and TNXL to correlate Ca²⁺ signal with morphological change. In this case, blebbing only occurred after the SOCE Ca²⁺ transient, with a typical 2–3 min duration, which was comparable to the duration of the SOCE Ca²⁺ transient (Figure 4E). This result was in contrast to the above results where a shorter transient resulted in a longer morphological change and is likely a property of the kinase cascade involved in regulating blebbing downstream of RhoA (Fackler and Grosse, 2008). Taken together, these results further demonstrate that CaR-Q can be activated by a variety of Ca²⁺-generating modules, and can be differentially regulated based on the spatial pattern of Ca²⁺ signaling. The experiments with Chr2 suggest that not only is Stim1-CaR-Q sensitive to plasma membrane Ca²⁺ but even more specifically is sensitive to a particular protein complex that is generating the Ca²⁺ influx.

Buffering Proteins Alter the Temporal Relationship between Ca²⁺ Signal and Morphology Change

The duration of blebbing morphology induced by the nAChR-α4 Ca²⁺ transient can be decreased using the cytoplasmic

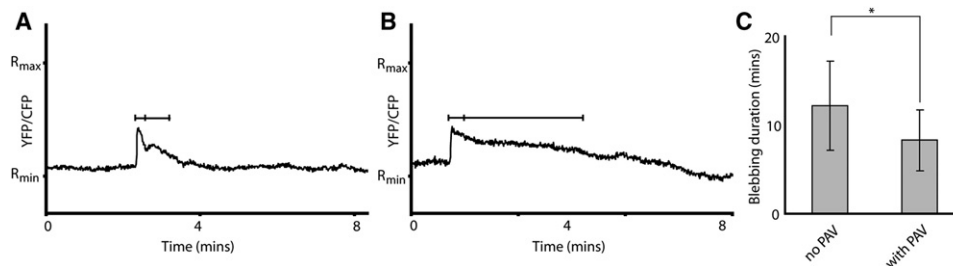


Figure 5. Effect of PAV on Blebbing Duration

(A) Representative ACh-induced Ca²⁺ transient in HEK293 cells expressing nAChR- α 4 and the TNXL biosensor. Typically, the peak duration was 10–20 s and the width of the shoulder (from end of peak to half maximum) was 30–40 s.

(B) Representative transient in HEK293 cells expressing nAChR- α 4, PAV-mRFP, and the TNXL biosensor. Typically, the peak duration was 20–30 s and the width of the shoulder was 1–2 min.

(C) Average duration of blebbing (time elapsed from onset of first bleb to retraction of all blebs) after ACh stimulation in cells expressing pLyn-CaR-Q, nAChR- α 4, and PAV, where indicated. The data are presented as the mean \pm standard deviation ($n = 12$ cells; * $p = 0.033$ by Student's t test).

Ca²⁺-buffering protein PAV (Schwaller et al., 2002) (Figure 5). We have observed that Ca²⁺ transients caused by SOCE or ionomycin that last several minutes result in shorter blebbing duration than Ca²⁺ transients that last several seconds, such as those caused by ACh or ATP. We sought to determine whether the characteristic output (i.e., blebbing morphology) duration of a given input could be changed by tuning the duration of the intermediate Ca²⁺ signal, either by shortening the SOCE transient or lengthening the nAChR- α 4 transient. When PAV (fused to mRFP or PAV-mRFP) was coexpressed with nAChR- α 4, the characteristic Ca²⁺ peak after ACh stimulation tended to be elongated by several seconds with an increased shoulder peak duration (Figures 5A and 5B), which is consistent with the role of PAV in buffering Ca²⁺ release and modulating the duration of Ca²⁺ transients (Schwaller et al., 2002). When PAV, nAChR- α 4, and pLyn-CaR-Q were coexpressed, the average duration of blebbing after ACh stimulation was significantly decreased from 12.2 ± 5.0 min without PAV to 8.3 ± 3.4 min ($n = 12$ cells, $p = 0.033$; Figure 5C). These results indicate that the Ca²⁺-responsive system presented here is sensitive to the duration of Ca²⁺ signal and that by tuning the duration of that signal, the duration of the morphology output can be tuned. However, it should be noted that there may be some effect of PAV on spatial buffering of the nAChR- α 4 Ca²⁺ signal that was not detected in our measurements.

CaR-Q-Regulated Morphology Changes Enhance Cell Migration

Blebbing morphology and cell migration can be controlled by light when a light-sensing module is present to generate a Ca²⁺ signal to regulate CaR-Q (Figure 6). Photoactivatable molecules are valuable research tools because they can be regulated with spatiotemporal precision, and photoactivatable proteins have been developed recently to control cell morphology and migration (Levskaia et al., 2009; Wu et al., 2009; Yeh et al., 2007) and DNA binding (Strickland et al., 2008). Several proteins exist that generate Ca²⁺ signals based on particular wavelengths of light (e.g., ChR2 with blue light [Petreanu et al., 2007] or VChR1 with green light [Zhang et al., 2008]) and may be suitable Ca²⁺-generating modules to activate CaR-Q. Indeed, cells coexpressing ChR2 and pLyn-CaR-Q developed a blebbing morphology

when exposed to flashing blue light (438/24 nm from a xenon lamp, 10 s period, 3% duty cycle) (Figure 6A). Given the role of actinomyosin contractility and blebbing in ameboid-like cell migration (Fackler and Grosse, 2008; Yang et al., 2006), we hypothesized that long-term activation of pLyn-CaR-Q would enable light-activated cell migration. Cells coexpressing pLyn-CaR-Q and ChR2 showed significant migration over 24 hr in a wound closure assay (Figures 6B–6K). The migration was significantly less when the ChR2 module was not present, when cells were incubated with Y-27632, or when the T19N mutant of pLyn-CaR-Q was used ($p < 0.001$, $n = 9$ wounds). Cells migrating into the wound tended to move as clusters, often with only one or two transfected cells per cluster of five to ten cells. This suggests that ameboid-like migration can direct cell migration in groups, which is supported by recent studies showing that photoactivation of Rac1 in a single cell can affect the direction of a cluster of adhered cells (Wang et al., 2010). This experiment demonstrates that light-activated cell migration can be achieved with an engineered Ca²⁺-signaling network by combining a light-sensitive module, ChR2, with a module that regulates a morphology known to be involved in migration, CaR-Q.

DISCUSSION

In this study, we have demonstrated the versatility and potential utility of engineered biomolecular systems based on Ca²⁺ signaling. In nature, Ca²⁺ signaling can simultaneously regulate many diverse cellular systems; cells are able to interpret the complexity of Ca²⁺ signaling because such signals are well defined in time (e.g., frequency and waveform; Berridge, 1998; De Koninck and Schulman, 1998) and space (through microdomains and buffering proteins; Schwaller et al., 2002; Wei et al., 2009), and because Ca²⁺-generating and Ca²⁺-responsive protein modules interact in different ways based on cell type or localization (Berridge et al., 2000). We showed that the CaR-Q protein could be activated by a variety of Ca²⁺-generating modules including nAChR- α 4, purinergic receptors, and the SOCE gate formed by Orai1 and Stim1. However, in each of these cases, CaR-Q was only functional when localized to the site of Ca²⁺ entry (PM or ER, respectively), showing that CaR-Q responds primarily to local Ca²⁺ signals. This is advantageous

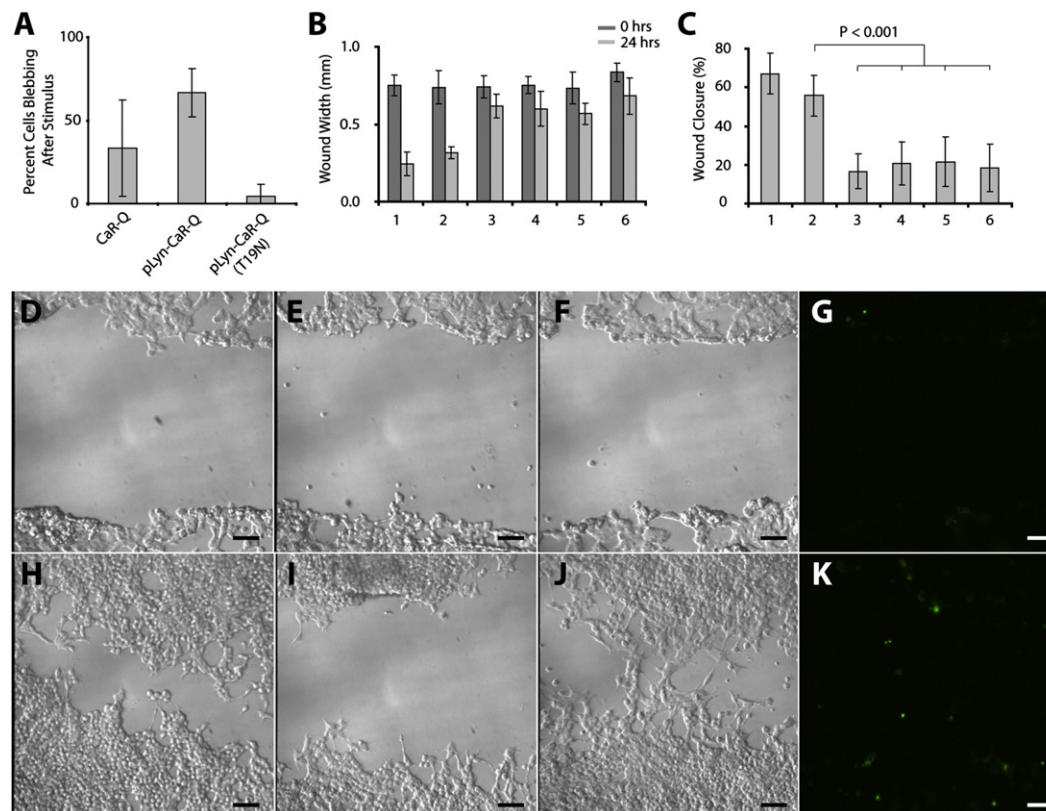


Figure 6. Light-Activated Cell Migration Using pLyn-CaR-Q and ChR2

(A) The percent of morphologically normal HEK293 cells that developed a blebbing morphology during flashing blue light illumination, under the indicated transfection and inhibitor conditions ($n = 3$ experiments each, >10 observed cells). Cells were cotransfected with ChR2-mCherry. Data are the mean and error bars are the standard deviation.

(B) Wound width immediately after wound (dark bars) and after 24 hr (light bars). (1) RhoA(DP)-YFP not illuminated, (2) pLyn-CaR-Q + ChR2 illuminated, (3) pLyn-CaR-Q(T19N) + ChR2 illuminated, (4) pLyn-CaR-Q + ChR2 + Y-27632 illuminated, (5) pLyn-CaR-Q illuminated, (6) pLyn-CaR-Q + ChR2 not illuminated.

(C) Data from (B) displayed as percent wound closure (initial width minus width at 24 hr divided by initial width) under the same conditions as in (B). The differences between condition 2 and conditions 3–6 were significant ($p < 0.001$). For (B) and (C), $n = 9$ experiments.

(D–K) Representative images from wound closure assays immediately after scraping (D–G) and 24 hr after scraping (H–K). HEK293 cells were expressing RhoA(DP)-YFP (D and H) or coexpressing ChR2 with pLyn-CaR-Q(T19N) (E and I) or pLyn-CaR-Q (F, G, J, and K). Bright-field and fluorescence images are presented for the same cells in the latter case (F and G at 0 hr, J and K at 24 hr). Scale bars represent 100 μm .

for an engineered system because it means that Ca²⁺ signaling need only be perturbed in part of the cell to activate CaR-Q.

Engineered proteins such as CaR-Q that respond to local Ca²⁺ signals may be useful tools to investigate the effect of local and global Ca²⁺ signaling in systems such as the NSCaTE element in Ca_v channels (Dick et al., 2008) or calpains, which are activated at Ca²⁺ concentrations not observed globally in the cytoplasm (Perrin and Huttenlocher, 2002). The ChR2 Ca²⁺-generating module was combined with pLyn-CaR-Q to enable photoactivation of the blebbing morphology, without making any changes to the CaR-Q module itself. We showed that long-term activation of the blebbing morphology increased cell motility and migration through a wound closure assay. At first pass, this appears to be in contrast to the generally accepted notion that overexpression of dominant-positive Rho proteins inhibits cell migration (Panopoulos et al., 2011; Xu et al., 2003). However, the salient feature of this experiment is that in the given context, activation of CaR-Q establishes the blebbing morphology, which is known to increase cell motility (Charras and Paluch, 2008). This result

was expected given the role of RhoA in blebbing and amoeboid-like cell migration (Fackler and Grosse, 2008; Yang et al., 2006). Even though there was no directed activation of CaR-Q, cells tended to migrate into the open space of the wound because they could not migrate into the monolayer.

This system may be further improved in the future to enable specific, direction-oriented cell migration either with a point-source light or perhaps by using a biochemical gradient with CaR-Q and a module that can translate a particular biochemical signal into a Ca²⁺ signal (e.g., EGF binding to EGFR; Tinhofer et al., 1996). Finally, the particular strategy employed here to enable allosteric, Ca²⁺-dependent control over RhoA may be a generalizable approach for engineering protein-level systems. The surface loop chosen to host the embedded IQ-motif peptide is present across the entire Ras GTPase family and may enable Ca²⁺-control studies in a variety of physiological systems. Whether the embedded peptide approach can be expanded beyond the Ras superfamily will depend on the careful selection of binding partners and structural analysis.

SIGNIFICANCE

We have developed a synthetic biosystem to control cell morphology and migration using Ca²⁺ signaling. Compelling reasons to use Ca²⁺ signaling in synthetic biosystems engineering are 3-fold. First, engineering a synthetic binding site in RhoA and changing the calmodulin-binding peptide (i.e., MLCK or IQ) enable the direction of the blebbing to be reversed from off-on to on-off. This shows that once a suitable site is identified in potentially any protein, we can make it turn on or off by changing the CaM-binding peptide. This shows the protein design versatility possible with Ca²⁺ signaling. Second, an emerging theme in Ca²⁺ signaling to explain how a ubiquitous Ca²⁺ signal can regulate so many diverse cellular events is the spatial localization of the Ca²⁺ signal. Using this knowledge, we created a system that can distinguish between local and global Ca²⁺ signals by targeting the RhoA chimera to the plasma membrane or endoplasmic reticulum so that it is only activated by plasma membrane Ca²⁺ fluxes or store-operated Ca²⁺ entry, respectively. This shows Ca²⁺-signaling specificity can be engineered. Third, Ca²⁺-mediated systems can exploit the inherent modularity of Ca²⁺ signaling to create multimodal systems where light and exogenous chemicals generated Ca²⁺ signals, which in turn activated the RhoA chimera. Three distinct modules were used to induce morphology changes, but many other modules are possible candidates for future applications including red-shifted opsins and appropriate cytokine receptors. This shows that pathway rewiring can be achieved by Ca²⁺ signaling. Engineering synthetic biological systems with input versatility and tunable spatiotemporal responses are key motivations for further applications of Ca²⁺ signaling in this field.

EXPERIMENTAL PROCEDURES

Plasmid Construction

CaR-Q, its derivative constructs, and other fusions were created by cloning with the pCfVtx3 vector as described previously (Truong et al., 2003). Primers used to amplify the 5' and 3' fragments of RhoA in CaR-Q are given in Supplemental Experimental Procedures. Plasmids encoding RhoA(Q63L), RBD, ChR2, Ora1, Stim1, and nAChR- $\alpha 4$ are Addgene plasmids 12968, 12602, 20938, 19756, 19754, and 15245, respectively. The dominant-negative mutant CaR-Q, RhoA (T19N), was created using the self-hybridizing overlap PCR method. The amino acid sequences of peptides used in this study are given in Supplemental Experimental Procedures.

Cell Culture and Transfection

COS7, HeLa, and HEK293 cells were maintained in Dulbecco's modified Eagle's medium supplemented with 25 mM D-glucose, 1 mM sodium pyruvate, and 4 mM L-glutamine (Invitrogen) in a T-25 flask. Cells were passaged at 95% confluency using 0.05% trypsin with EDTA (Sigma-Aldrich) and seeded onto glass-bottom dishes at 1:15 dilution (Mattek). Cells were transiently transfected using Lipofectamine 2000 according to the manufacturer's directions (Invitrogen).

Reagents

Cells treated with Y-27632 (5 μ M) and CDZ (50 μ M) were preincubated with inhibitor in PBS with CaCl₂ for 1 hr prior to imaging. ATP (10 μ M), ACh (1 mM), ionomycin (1 μ M), and Tg (2 μ M; BioShop) were added by diluting 1:10 in imaging medium (PBS with CaCl₂, except where noted otherwise) after a 5 min control period. Rhodamine-phalloidin (Invitrogen) was used according to the manufacturer's protocol. The Ca²⁺-buffering kit was used according to

the manufacturer's protocols (Biotium). All reagents, except where noted, were from Sigma.

Illumination, Imaging, and Wound Assay

Imaging was performed using an inverted IX81 microscope with a Lambda DG4 xenon lamp source and QuantEM 512SC CCD camera with a 20 \times , 40 \times , and 100 \times oil immersion or 10 \times objectives (Olympus). Filter excitation (ex) and emission (em) band-pass specifications were as follows: for CFP, ex: 438/24 nm, em: 482/32 nm; for YFP, ex: 500/24 nm, em: 542/27 nm; for RFP, ex: 580/20 nm, em: 630/60 nm (Semrock). For ChR2, excitation was done using the CFP excitation filter normally with a 300 ms flash every 10 s. FRET emissions were recorded by simultaneously imaging the CFP and YFP channels using a DualView SpecEM system (Olympus). Image acquisition was done with MetaMorph Advanced (Olympus).

Most imaging experiments were conducted in PBS with CaCl₂, except SOCE experiments, where CaCl₂ was added to Ca²⁺-free PBS after Tg, and ChR2 experiments, where complete growth medium was used. Wound assays were conducted by growing transfected HEK293 cells to confluency, scraping the dish with a 1 μ l pipette tip, washing three times in PBS, and incubating in complete growth medium overnight. Overnight illumination was provided using an iPod programmed to flash blue light for 1 s every 15 s. The power output of the iPod display was measured at 0.80 mW/cm² for white light and 0.12 mW/cm² for blue light (450 nm) using a Konica-Minolta CS-200 spectroradiometer (DisplayMate) in a dark room with the iPod running on AC power. The power output of the xenon lamp at the microscope stage is 25 mW/cm². For TNXL biosensor experiments, 1 μ M ionomycin was added at the end of experiments to establish R_{max} and then 2 mM EDTA was added to establish R_{min}.

Data Analysis

A cell was counted as blebbing if at least one circular bleb appeared at any point within 20 min of stimulus onset, unless it was also blebbing before stimulation, in which case a cell was not considered. Data regarding the frequency of cell blebbing after a stimulus are the mean of at least three independent experiments over at least ten cells. Data regarding the frequency of cell blebbing before stimulus are the mean of at least ten independent experiments over at least 100 cells. Data are presented as the mean \pm standard deviation. Significance, where discussed, was determined using an independent Student's t test and $p < 0.05$ was considered significant.

PC values for image correlation between pLyn-CaR-Q and RBD-mRFP-GST were calculated using MetaMorph. Images were cropped to remove nontransfected cells, and the background was subtracted using a 32 \times 32 pixel square median filter. Cropped, background-subtracted images were used for PC calculation without any further processing.

Curve fitting for EC₅₀ estimation was done using MS Excel by minimizing the sum of squares between the generic sigmoid of the form shown in Figure 2 and the data collected in Figure 2. The squared Pearson correlation coefficient (r^2) was calculated by comparing the values of the data and the best fit.

SUPPLEMENTAL INFORMATION

Supplemental Information includes Supplemental Experimental Procedures, three figures, and eight movies and can be found with this article online at doi:10.1016/j.chembiol.2011.09.014.

ACKNOWLEDGMENTS

This work was made possible by plasmid sharing through Addgene. This work was supported by a fellowship to E.M. from the Natural Science and Engineering Research Council and a grant to K.T. from the Canadian Institutes of Health Research (81262). E.M. designed and carried out all experiments, analyzed the data, and wrote the manuscript. K.T. conceived the embedded peptide strategy, provided guidance, and helped write the manuscript.

Received: June 13, 2011

Revised: September 6, 2011

Accepted: September 19, 2011

Published: December 22, 2011

REFERENCES

- Berridge, M.J. (1993). Inositol trisphosphate and calcium signalling. *Nature* 367, 315–325.
- Berridge, M.J. (1998). Neuronal calcium signaling. *Neuron* 21, 13–26.
- Berridge, M.J., Lipp, P., and Bootman, M.D. (2000). The versatility and universality of calcium signalling. *Nat. Rev. Mol. Cell Biol.* 1, 11–21.
- Charras, G., and Paluch, E. (2008). Blebs lead the way: how to migrate without lamellipodia. *Nat. Rev. Mol. Cell Biol.* 9, 730–736.
- Correia, S.S., Bassani, S., Brown, T.C., Lisé, M.F., Backos, D.S., El-Husseini, A., Passafaro, M., and Esteban, J.A. (2008). Motor protein-dependent transport of AMPA receptors into spines during long-term potentiation. *Nat. Neurosci.* 11, 457–466.
- Crivici, A., and Ikura, M. (1995). Molecular and structural basis of target recognition by calmodulin. *Annu. Rev. Biophys. Biomol. Struct.* 24, 85–116.
- De Koninck, P., and Schulman, H. (1998). Sensitivity of CaM kinase II to the frequency of Ca²⁺ oscillations. *Science* 279, 227–230.
- Dick, I.E., Tadross, M.R., Liang, H., Tay, L.H., Yang, W., and Yue, D.T. (2008). A modular switch for spatial Ca²⁺ selectivity in the calmodulin regulation of CaV channels. *Nature* 457, 830–834.
- Fackler, O.T., and Grosse, R. (2008). Cell motility through plasma membrane blebbing. *J. Cell Biol.* 181, 879–884.
- Gray, D.C., Mahrus, S., and Wells, J.A. (2010). Activation of specific apoptotic caspases with an engineered small-molecule-activated protease. *Cell* 142, 637–646.
- Hakoshima, T., Shimizu, T., and Maesaki, R. (2003). Structural basis of the Rho GTPase signaling. *J. Biochem.* 134, 327–331.
- Kalos, M., Levine, B.L., Porter, D.L., Katz, S., Grupp, S.A., Bagg, A., and June, C.H. (2011). T cells with chimeric antigen receptors have potent antitumor effects and can establish memory in patients with advanced leukemia. *Sci. Transl. Med.* 3, 95ra73.
- Levsikaya, A., Weiner, O.D., Lim, W.A., and Voigt, C.A. (2009). Spatiotemporal control of cell signalling using a light-switchable protein interaction. *Nature* 461, 997–1001.
- Lukas, T.J., Burgess, W.H., Prendergast, F.G., Lau, W., and Watterson, D.M. (1986). Calmodulin binding domains: characterization of a phosphorylation and calmodulin binding site from myosin light chain kinase. *Biochemistry* 25, 1458–1464.
- Mank, M., Reiff, D.F., Heim, N., Friedrich, M.W., Borst, A., and Griesbeck, O. (2006). A FRET-based calcium biosensor with fast signal kinetics and high fluorescence change. *Biophys. J.* 90, 1790–1796.
- Mills, E., Pham, E., and Truong, K. (2010). Structure based design of a Ca²⁺-sensitive RhoA protein that controls cell morphology. *Cell Calcium* 48, 195–201.
- Nashmi, R., Dickinson, M.E., McKinney, S., Jareb, M., Labarca, C., Fraser, S.E., and Lester, H.A. (2003). Assembly of $\alpha 4\beta 2$ nicotinic acetylcholine receptors assessed with functional fluorescently labeled subunits: effects of localization, trafficking, and nicotine-induced upregulation in clonal mammalian cells and in cultured midbrain neurons. *J. Neurosci.* 23, 11554–11567.
- Palmer, A.E., Giacomello, M., Kortemme, T., Hires, S.A., Lev-Ram, V., Baker, D., and Tsien, R.Y. (2006). Ca²⁺ indicators based on computationally redesigned calmodulin-peptide pairs. *Chem. Biol.* 13, 521–530.
- Panopoulos, A., Howell, M., Fotedar, R., and Margolis, R.L. (2011). Glioblastoma motility occurs in the absence of actin polymer. *Mol. Biol. Cell* 22, 2212–2220.
- Perrin, B.J., and Huttenlocher, A. (2002). Calpain. *Int. J. Biochem. Cell Biol.* 34, 722–725.
- Pertz, O., Hodgson, L., Klemke, R.L., and Hahn, K.M. (2006). Spatiotemporal dynamics of RhoA activity in migrating cells. *Nature* 440, 1069–1072.
- Peteanu, L., Huber, D., Sobczyk, A., and Svoboda, K. (2007). Channelrhodopsin-2-assisted circuit mapping of long-range callosal projections. *Nat. Neurosci.* 10, 663–668.
- Rekas, A., Alattia, J.R., Nagai, T., Miyawaki, A., and Ikura, M. (2002). Crystal structure of Venus, a yellow fluorescent protein with improved maturation and reduced environmental sensitivity. *J. Biol. Chem.* 277, 50573–50578.
- Robinson, D.N., Cavet, G., Warrick, H.M., and Spudich, J.A. (2002). Quantitation of the distribution and flux of myosin-II during cytokinesis. *BMC Cell Biol.* 3, 4.
- Schwaller, B., Meyer, M., and Schiffmann, S. (2002). 'New' functions for 'old' proteins: the role of the calcium-binding proteins calbindin D-28k, calretinin and parvalbumin, in cerebellar physiology. *Studies with knockout mice. Cerebellum* 1, 241–258.
- Strickland, D., Moffat, K., and Sosnick, T.R. (2008). Light-activated DNA binding in a designed allosteric protein. *Proc. Natl. Acad. Sci. USA* 105, 10709–10714.
- Tinhofer, I., Maly, K., Dietl, P., Hochholderinger, F., Mayr, S., Obermeier, A., and Grunicke, H.H. (1996). Differential Ca²⁺ signaling induced by activation of the epidermal growth factor and nerve growth factor receptors. *J. Biol. Chem.* 271, 30505–30509.
- Truong, K., Khorchid, A., and Ikura, M. (2003). A fluorescent cassette-based strategy for engineering multiple domain fusion proteins. *BMC Biotechnol.* 3, 8.
- Trybus, K.M., Gushchin, M.I., Lui, H., Hazelwood, L., Kremntsova, E.B., Volkman, N., and Hanein, D. (2007). Effect of calcium on calmodulin bound to the IQ motifs of myosin V. *J. Biol. Chem.* 282, 23316–23325.
- Wang, X., He, L., Wu, Y.I., Hahn, K.M., and Montell, D.J. (2010). Light-mediated activation reveals a key role for Rac in collective guidance of cell movement in vivo. *Nat. Cell Biol.* 12, 591–597.
- Wei, C., Wang, X., Chen, M., Ouyang, K., Song, L.S., and Cheng, H. (2009). Calcium flickers steer cell migration. *Nature* 457, 901–905.
- Wu, Y.I., Frey, D., Lungu, O.I., Jaehrig, A., Schlichting, I., Kuhlman, B., and Hahn, K.M. (2009). A genetically encoded photoactivatable Rac controls the motility of living cells. *Nature* 461, 104–108.
- Xu, J., Wang, F., Van Keymeulen, A., Herzmark, P., Straight, A., Kelly, K., Takuwa, Y., Sugimoto, N., Mitchison, T., and Bourne, H.R. (2003). Divergent signals and cytoskeletal assemblies regulate self-organizing polarity in neutrophils. *Cell* 114, 201–214.
- Yang, N.Y., Pasquale, E.B., Owen, L.B., and Ethell, I.M. (2006). The EphB4 receptor-tyrosine kinase promotes the migration of melanoma cells through Rho-mediated actin cytoskeleton reorganization. *J. Biol. Chem.* 281, 32574–32586.
- Yeh, B.J., Rutigliano, R.J., Deb, A., Bar-Sagi, D., and Lim, W.A. (2007). Rewiring cellular morphology pathways with synthetic guanine nucleotide exchange factors. *Nature* 447, 596–600.
- Zhang, F., Prigge, M., Beyrière, F., Tsunoda, S.P., Mattis, J., Yizhar, O., Hegemann, P., and Deisseroth, K. (2008). Red-shifted optogenetic excitation: a tool for fast neural control derived from *Volvox carterii*. *Nat. Neurosci.* 11, 631–633.
- Zhou, Y., Meraner, P., Kwon, H.T., Machnes, D., Oh-hora, M., Zimmer, J., Huang, Y., Stura, A., Rao, A., and Hogan, P.G. (2010a). STIM1 gates the store-operated calcium channel ORAI1 in vitro. *Nat. Struct. Mol. Biol.* 17, 112–116.
- Zhou, Y., Ramachandran, S., Oh-hora, M., Rao, A., and Hogan, P.G. (2010b). Pore architecture of the ORAI1 store-operated calcium channel. *Proc. Natl. Acad. Sci. USA* 107, 4896–4901.